

# NIR-II window imaging to assess the impact of inherited Notch-Dll4 expression on pulmonary radiation injury

<sup>1</sup>Mir Hadi Razeghi Kondelaji, <sup>2</sup>Guru Prasad Sharma, <sup>3</sup>Jaidip Jagtap, <sup>1</sup>Christopher Hansen, <sup>2</sup>Tracy Gasperetti, <sup>2</sup>Brian L. Fish, <sup>2</sup>Heather A. Himgung, <sup>1</sup>Amit Joshi

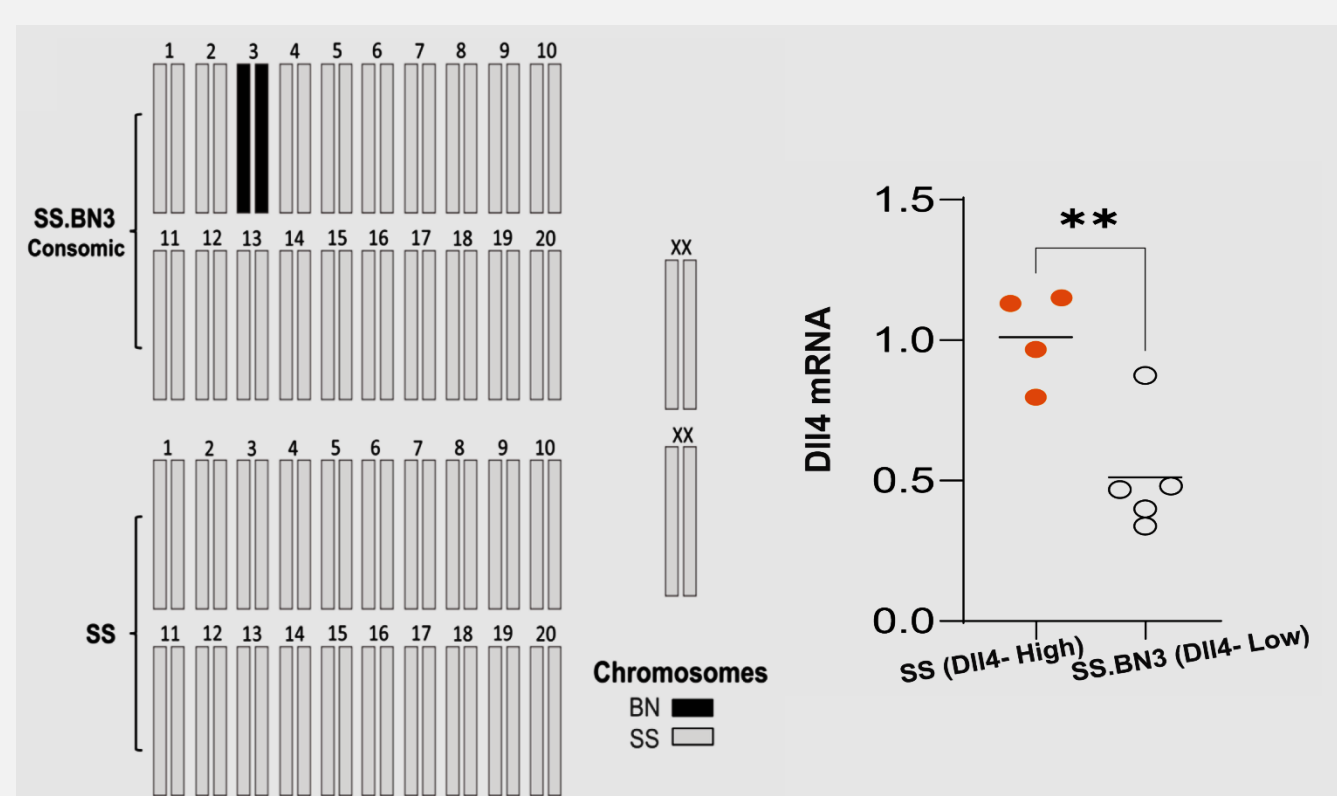
<sup>1</sup>Department of Biomedical Engineering, <sup>2</sup>Department of Radiation Oncology, Medical College of Wisconsin, Milwaukee, WI 53266

<sup>3</sup>Department of Radiology, Mayo Clinic, Rochester, MN

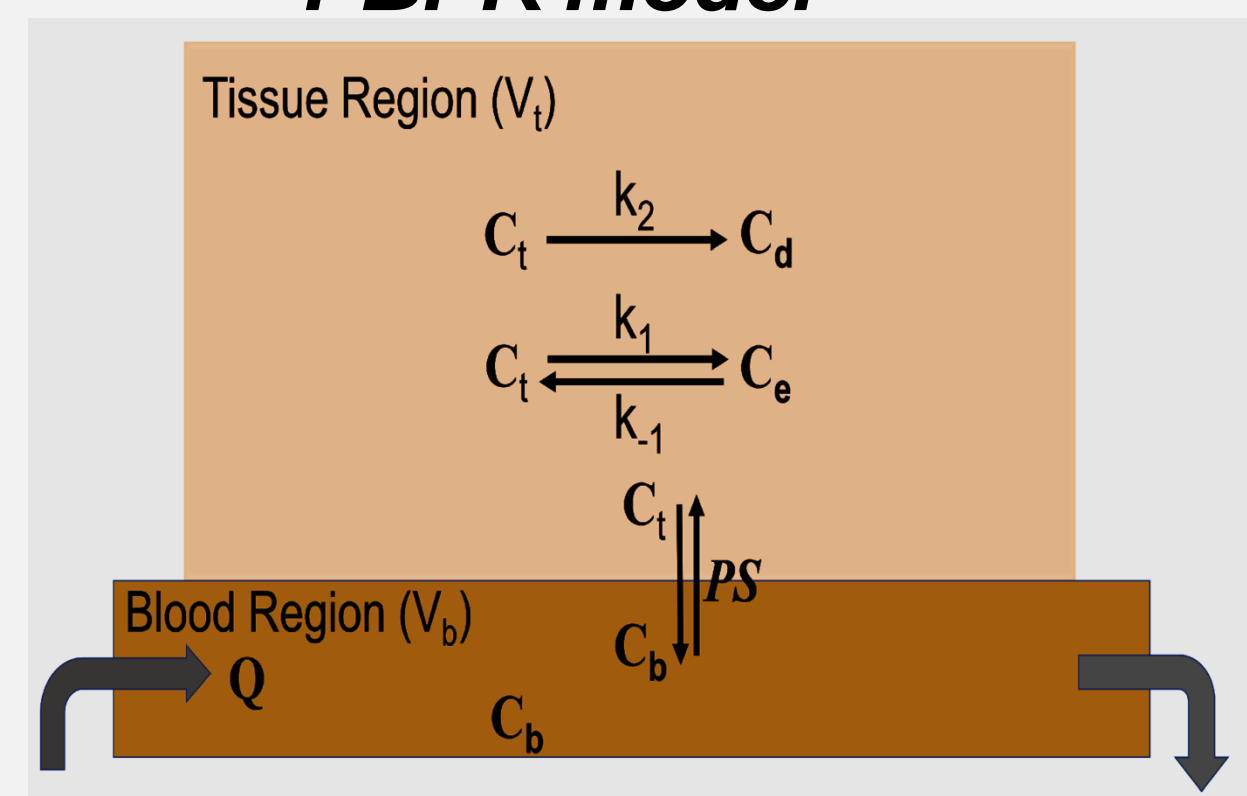
## Introduction

- There is a lifetime risk for survivors of high-dose radiation exposure to develop late multi-organ damage which is known as delayed Effects of acute radiation exposure (DEARE).
- Our group has demonstrated increased permeability of vessels in lungs of rats 6 weeks after irradiation (Jaidip Jagtap and et al, 2021)
- Dll4 is an endothelial-specific Notch ligand which is necessary for normal vascular development.
- We employed consomic rat model with natively reduced Dll4 expression (Flister et al 2014, Flister et al 2017) to evaluate the impact of Dll4 on radiation induced vascular changes.
- Prior works suggest significant changes (reduction) in tumor angiogenesis in cases with reduced Dll4 expression (Dll4-Low) (Sharma G. et al 2020, and Flister M. et al 2017).
- In the consomic model, the third chromosome in the Dahl-SS rat is substituted with chromosome 3 from the Brown Norway rat with lower Dll4 expression.
- In this study, we have evaluated the susceptibility of SS.BN3 (Dll4-low) rats to progressive radiation-induced vascular dysfunction.
- We have used Near Infrared Region (NIR) second window imaging to non-invasively track any changes in vascular permeability of lung and kidney.
- We used FDA-cleared dye, Indocyanine Green (ICG), which completely avoids tissue background autofluorescence and reduces scattering.
- We used imaging-based Pharmacokinetic model combined with novel imaging to investigate the role of Dll4 expression in our DEARE model.

### Consomic model



### PBPK model



## Methods

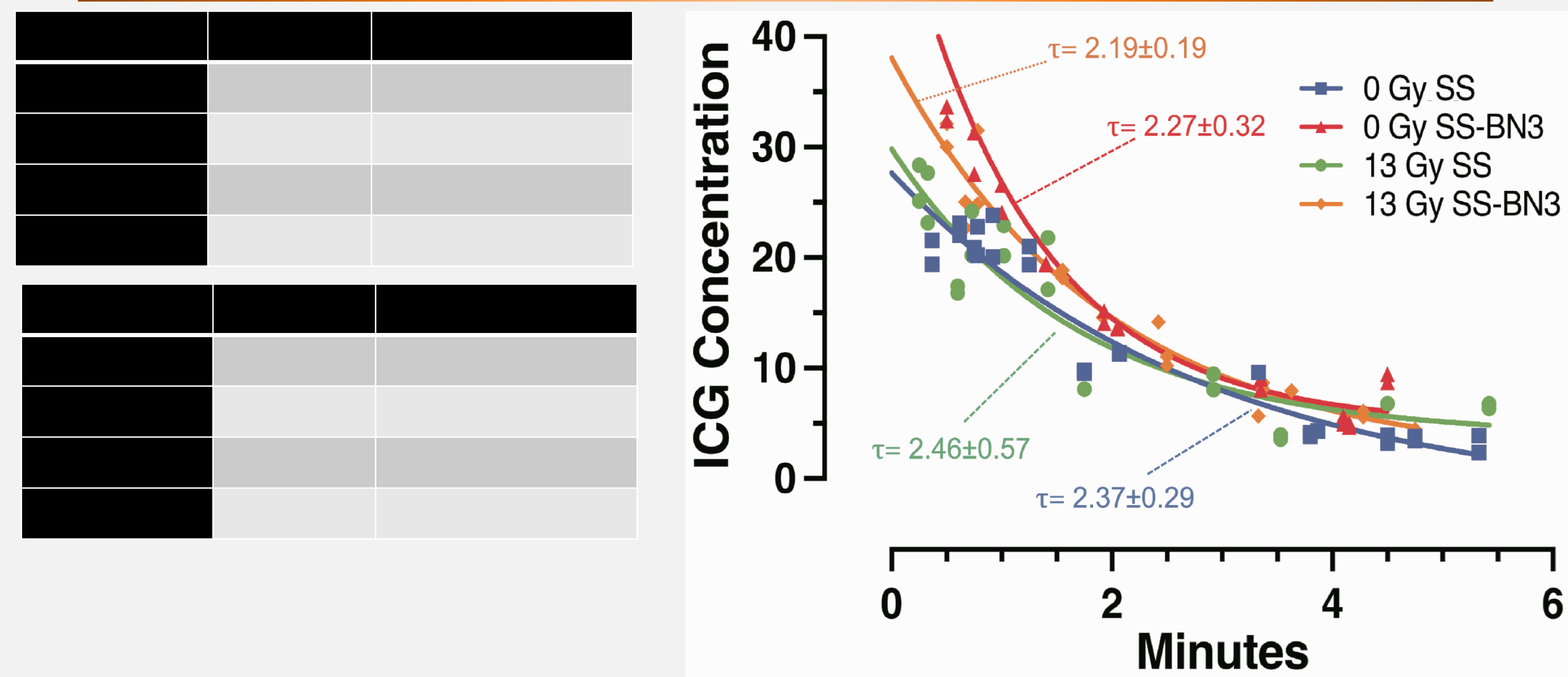


**Figure 1.** Physiology-Based Pharmacokinetic Modeling (PBPK) parameters (left) and the ICG decay lifetime was computed by fitting the last equation (right), while  $S_p=0$  for all 4 groups (n=5 for SS and n=4 for SS.BN3 rats).

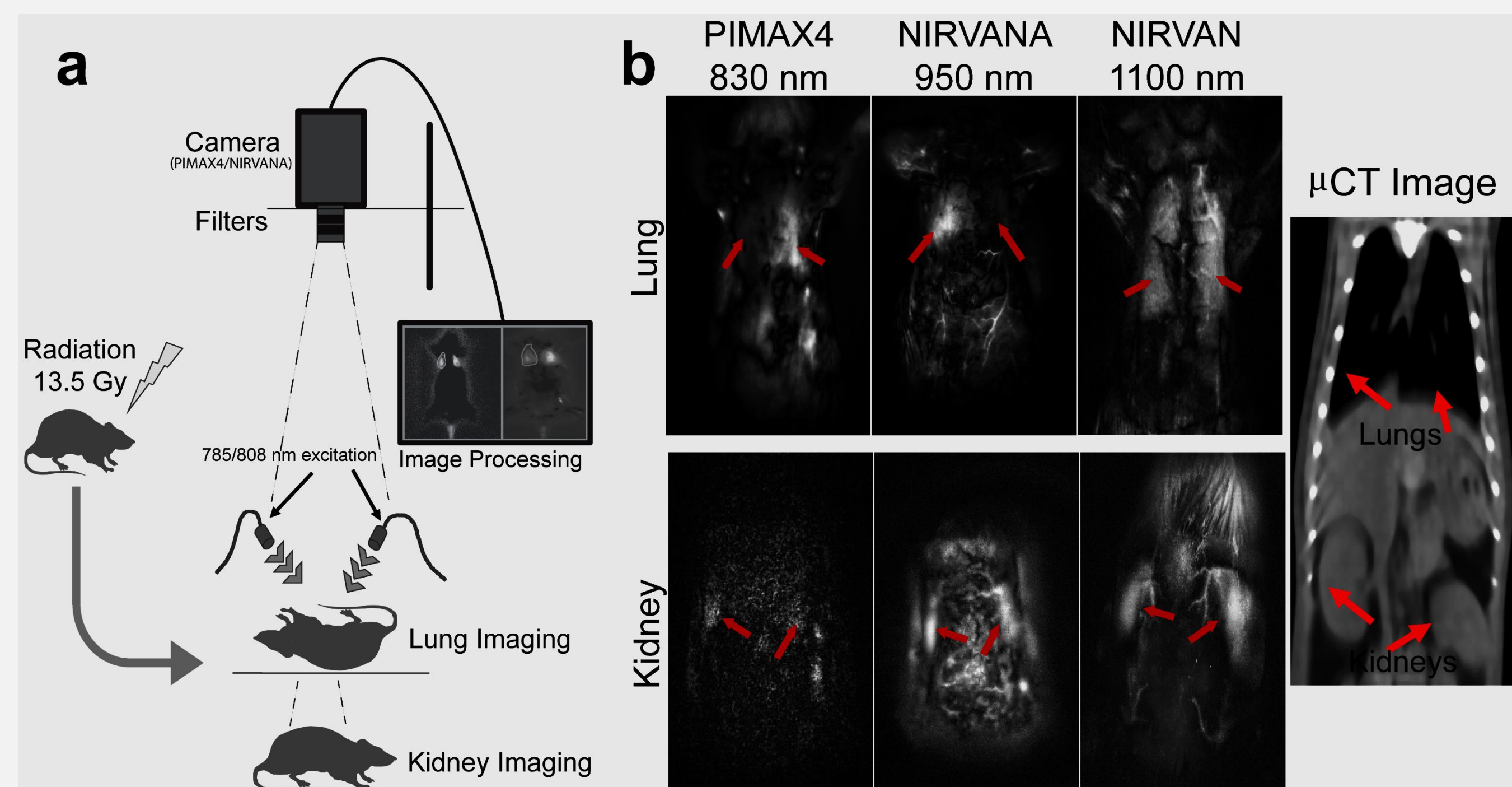


**Figure 2.** Imaging setup and image processing technique. (a) NIR Fluorescence imaging setup using Indocyanine Green optical imaging for lung and kidney 42 and 90 days after PBI. (b) Determination of region of interest (ROI) for lung and kidney using principal component analysis (PCA) for 3 different camera setups. Reference Lung and kidney locations have been illustrated by using a cross-sectional CT image of a representative SS rat via the SmART 225 kV orthovoltage x-ray system (Precision X-Ray, North Branford, Connecticut) at 40 kV and 5 mA with 0.2 mm voxels.

## Methods

PBPK model

$$\begin{aligned}
 V_b \frac{dC_b}{dt} &= F((1 - \alpha)C_{in} - C_b) + PS(C_t - C_b) \\
 V_t \frac{dC_t}{dt} &= PS(C_b - C_t) + V_t(k_{-1}C_e - (k_1 + k_2)C_t) \\
 V_t \frac{dC_e}{dt} &= V_t(k_1C_t - k_{-1}C_e) \\
 V_t \frac{dC_d}{dt} &= V_t(k_2C_t) \\
 V_b \frac{dC_B}{dt} &= F(\alpha C_{in} - C_B) \\
 \frac{dC_{in}}{dt} &= \left(\frac{d_0}{BV}\right) \times S_p - \left(\frac{C_{in}}{\tau}\right), \text{ for } t > T_{inj}, S_p = 0
 \end{aligned}$$

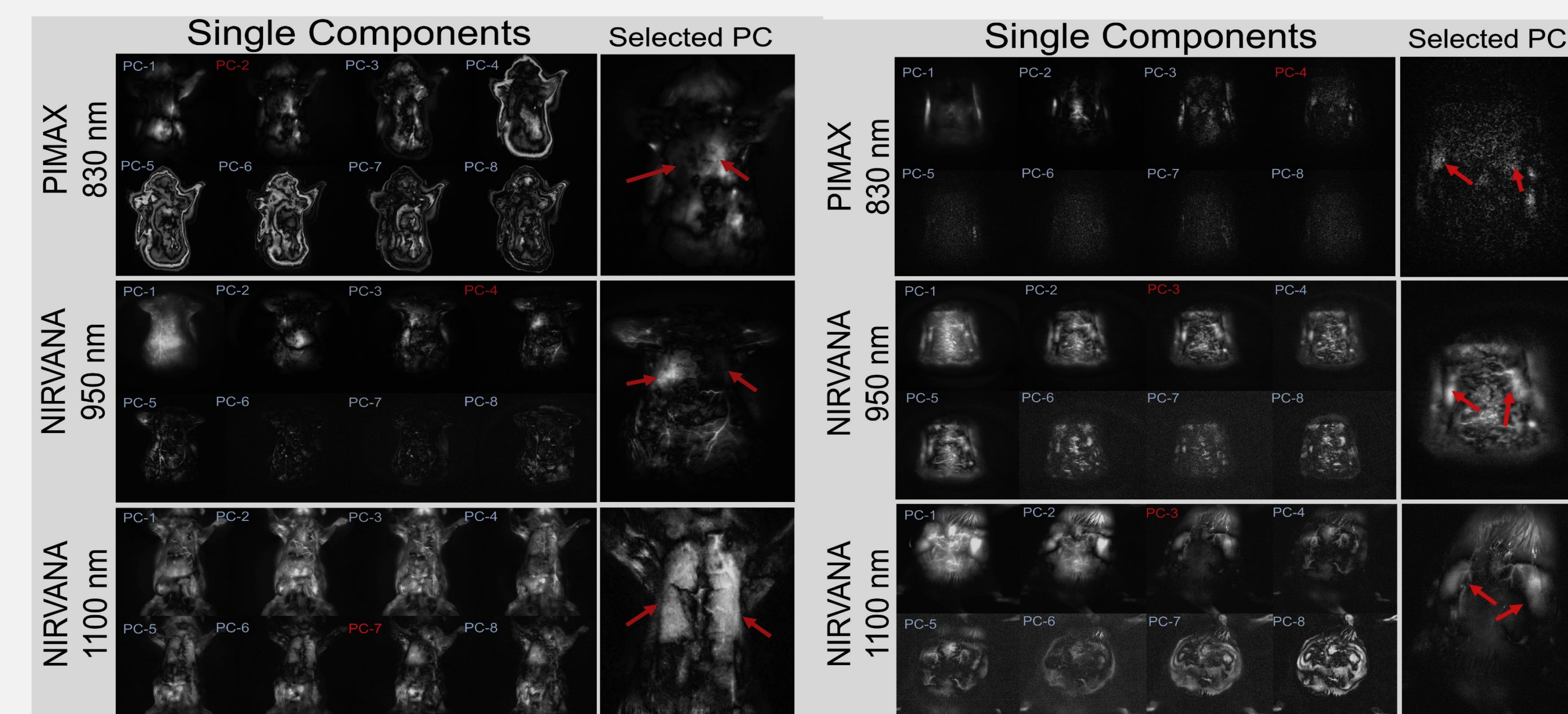


**Figure 3.** The principal component analysis (PCA) of 3 different imaging setups. Imaging data were used to data decomposition based on PCA to discriminate different organs. For each setup the best component was used for lung and kidney segmentation. NIR-2 window represents more clear and robust organ decomposition by PCA technique. The 1100 nm long pass filter with 808 laser excitation represents the most prominent lung and kidney segments. The selected components are shown by a red arrow.

## Results

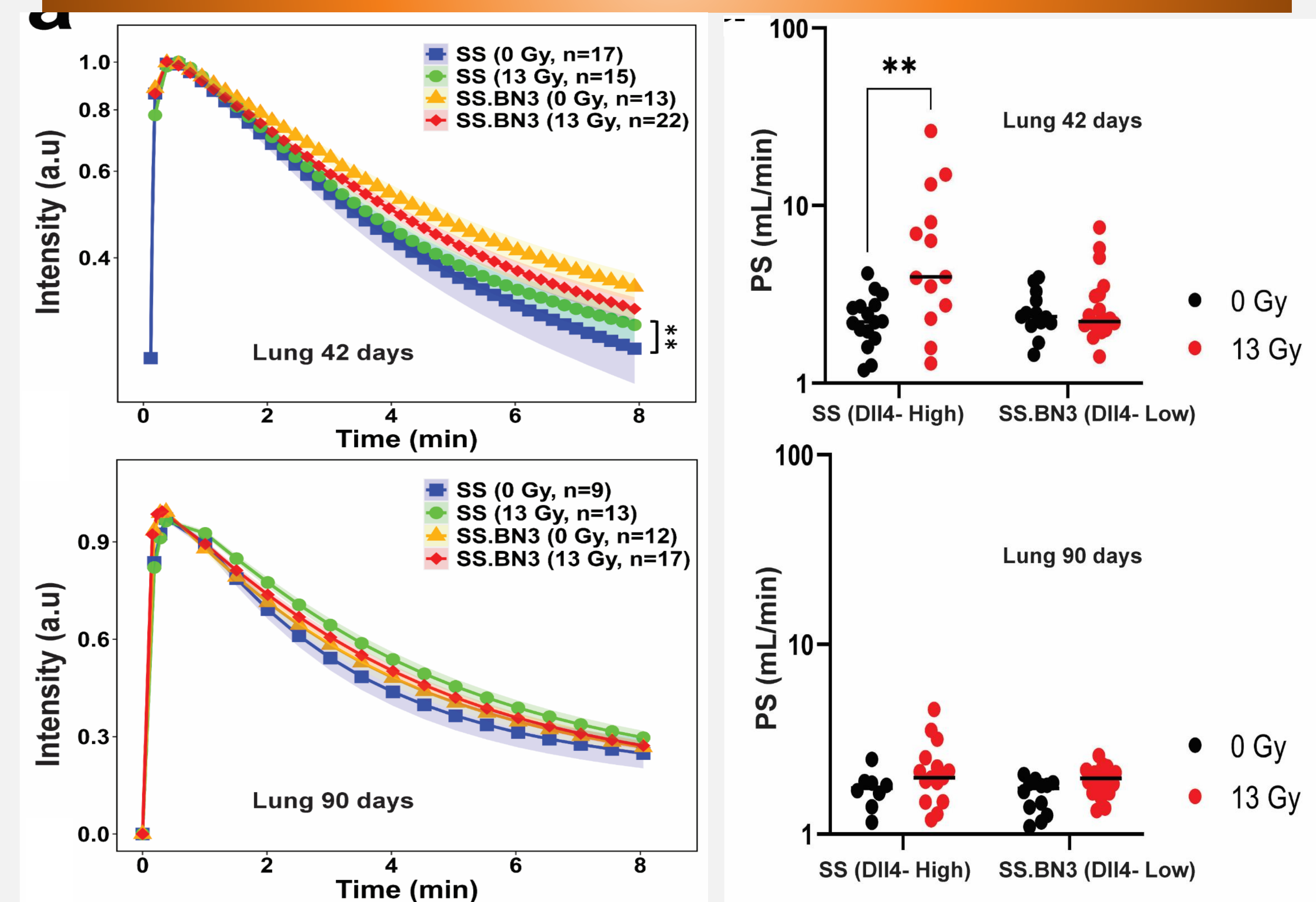


**Figure 4.** SS.BN3 (Dll4-low) rats are protected from radiation-induced increases in lung vascular permeability. (a) Kinetics of ICG uptake and clearance in the right lung at 42 days (a total of 32 SS and 35 SS.BN3 rats, i.e., SS 0 Gy (n=17), SS 13 Gy (n=15), SS.BN3 0 Gy (n=13), and SS.BN3 13 Gy (n=22) (b) ICG fluorescence kinetics of right lung at 90 days following PBI (a total of 22 SS and 29 SS.BN3 rats, i.e., SS 0 Gy (n=9), SS 13 Gy (n=13), SS.BN3 0 Gy (n=12), and SS.BN3 13 Gy (n=17)). (d) The PS, permeability-surface area product in the right lung at 42 days and 90 days (representing in the a and b) post PBI. Data points represent the mean for each experimental group with the 90% confidence interval shown in the color-matched highlighted area (\*\*P<0.01, two-way ANOVA Sidak's multiple testing correction).

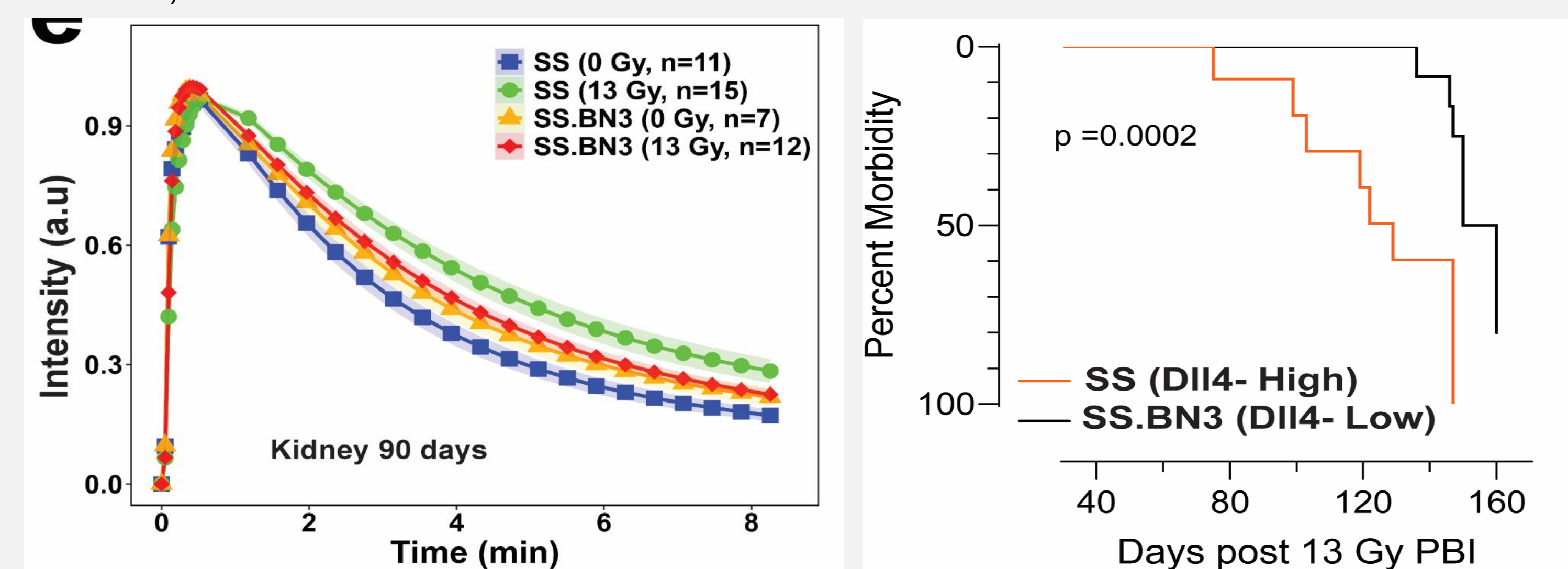


**Figure 5.** (a) ICG fluorescence kinetics in the right kidney at 90 after PBI (a total of 16 SS and 19 SS.BN3 rats, i.e., SS 0 Gy (n=11), SS 13 Gy (n=15), SS.BN3 0 Gy (n=7), and SS.BN3 13 Gy (n=12)). (b) The survival following 13 Gy partial body irradiation (PBI) in adult SS (n=13) and SS.BN3 rats (n=19). P-value for log-rank analysis: p = 0.0002 for SS vs SS.BN3 following 13Gy PBI.

## Conclusion

Our study suggests a significant dependence of radiation induced vascular injury on the inherited notch-DLL4 expression, which can be imaged in 200g rats with NIR 2<sup>nd</sup> window imaging.

## Acknowledgment

This work was supported by funding from NIH/NIAID U01A1133594, U01A1138331, NIH/NCI 2R01CA193343 the MCW Department of Radiation Oncology, and the MCW Cancer Center.